Relationship between Mode Specific and Thermal Unimolecular Rate Constants for HOCl → OH + Cl Dissociation†

Kihyung Song, Lipeng Sun, and William L. Hase*

Department of Chemistry and Institute for Scientific Computing, Wayne State University, Detroit, Michigan 48202-3489

S. Yu. Grebenshchikov and Reinhard Schinke

Max-Planck-Institut für Strömungsforschung, Bunsenstrasse 10, D-37073 Göttingen, Germany

Received: December 31, 2001; In Final Form: May 6, 2002

Recent quantum dynamical calculations [Hauschildt, J.; et al. *Chem. Phys. Lett.* **1999**, *300*, 569] have shown that HOCl → OH + Cl dissociation on the ground-state potential energy surface, and for $J = 0$, occurs predominantly via isolated compound-state resonances, whose rates are highly mode-specific. In this work, these resonance rates are averaged to calculate the HOCl → OH + Cl unimolecular rate constant as a function of temperature and pressure. The result is compared with the standard pressure and temperature dependent RRKM unimolecular rate constant. It is found that the state-specificity makes the pressure-dependent rates significantly lower than the RRKM rates in the intermediate pressure regime.

I. Introduction

At the microscopic, elementary level, unimolecular dissociation[1,2] may be described in terms of isolated[3−8] or overlapping[9−12] resonance states, each with a specific unimolecular rate constant k_n. The resonance line width Γ_n and lifetime τ_n are related to k_n by

$$k_n = \Gamma_n/\hbar = 1/\tau_n \tag{1}$$

The resonance states are said to be isolated if the widths of their lines are small compared with the distances between them; that is, $\Gamma_n \ll 1/\rho(E)$, where $\rho(E)$ is the density of states for the energized molecule. As the line widths broaden and/or the number of resonance states in an energy interval increases, the spectrum of the molecule may no longer be quasidiscrete, because the resonance lines may overlap.[9−12]

Following the pioneering work of Rabinovitch and Setser,[1] the collision-averaged unimolecular dissociation of a monoenergetically excited molecule in a chemical activation or photoactivation experiment may be interpreted by the mechanism[1]

$$\begin{aligned} \mathrm{A}^* &\xrightarrow{k(\omega,E)} \text{decomposition products (D)} \\ &\xrightarrow{\omega} \text{stabilized reactants (S)} \end{aligned} \tag{2}$$

where ω is the collision frequency and the unimolecular rate constant is given by[1]

$$k(\omega,E) = \omega D/S \tag{3}$$

According to RRKM theory,[1,2] the dissociation of monoenergetically excited molecules is random with exponential decay, so that $k(\omega,E)$ equals the RRKM rate constant $k(E)$. However, if the dissociation occurs via N_o isolated resonance states in the energy interval $E \rightarrow E + \Delta E$, $k(\omega,E)$ is pressure dependent and may be written as[13−15]

$$k(\omega,E) = N_0/\{\sum 1/(k_n + \omega)\} - \omega \tag{4}$$

with the high and low-pressure limits of

$$k(\infty,E) = \langle k_n \rangle \tag{5}$$

$$k(0,E) = \langle 1/k_n \rangle^{-1} \tag{6}$$

Resonance states with small rate constants contribute more to $k(\omega,E)$ as the pressure is lowered, so that $k(\omega,E)$ decreases with decrease in pressure.

The monoenergetic unimolecular rate constant $k_{uni}(\omega,E)$ in the Lindemann−Hinshelwood mechanism for thermal unimolecular decomposition is related to the above $k(\omega,E)$ by[6,15−17]

$$k_{uni}(\omega,E) = \frac{\omega k(\omega,E)}{k(\omega,E) + \omega} \tag{7}$$

If eq 4 is used for $k(\omega,E)$, eq 7 becomes

$$k_{uni}(\omega,E) = \frac{\omega}{N_0}\sum_n \frac{k_n}{k_n + \omega} \tag{8}$$

where the summation is over the N_0 resonance states within $E \rightarrow E + \Delta E$. The high- and low-pressure limits of $k_{uni}(\omega,E)$ are $\langle k_n \rangle$ and ω, respectively. By summing over all of the resonance states, with the appropriate Boltzmann weighting, the following expression for the thermal Lindemann−Hinshelwood unimolecular rate constant is obtained:

$$k_{uni}(\omega,T) = \frac{\omega}{Q}\sum_n \frac{k_n \exp(-E_n/k_B T)}{k_n + \omega} \tag{9}$$

† Part of the special issue "Donald Setser Festschrift".

* To whom correspondence should be addressed.

10.1021/jp014689l CCC: $22.00
Published on Web 06/20/2002

where Q is the partition function for the reactant molecule's internal degrees of freedom. If the energy E can be assumed to be continuous,[15,18] one obtains $k_{uni}(\omega,T)$ by Boltzmann weighting the $k_{uni}(\omega,E)$ given by eq 7; i.e.

$$k_{uni}(\omega,T) = \frac{\omega}{Q}\int_0^\infty \frac{k(\omega,E)\rho(E)\exp(-E/k_BT)}{k(\omega,E)+\omega}\,dE \qquad (10)$$

This expression is a further extension of the standard thermal Lindemann-Hinselwood unimolecular rate constant,[2] for it incorporates the standard RRKM model in which $k(\omega,E)$ equals the RRKM rate constant $k(E)$ as well as eq 4, the isolated resonance model for $k(\omega,E)$. In the low-pressure limit, both the RRKM and isolated resonance models give the same expression for $k_{uni}(\omega,T)$; i.e., it is proportional to ω and the Boltzmann-weighted density of states of reacting molecules. In addition, if the average $\langle k_n \rangle$ of the resonance rate constants in the energy interval $E \rightarrow E + \Delta E$ equals the RRKM rate constant $k(E)$, the RRKM and isolated resonance models also give the same rate constant in the high-pressure limit. Thus, for this case, the $k_{uni}(\omega,T)$ of the two models may only differ in the intermediate pressure regime.

In previous work,[19] the above equations were used to calculate thermal rate constants for

$$HO_2 \rightarrow H + O_2 \qquad (11)$$

dissociation. Quantum dynamical calculations show that HO_2 dissociates via resonance states whose wave functions have random characteristics and appear to be unassignable.[20−24] Thus, though the resonance rates are state-specific, they are not mode-specific.[6] Furthermore, the calculated rate constants[22] appear to be statistical state-specific and in accord with the Porter-Thomas $P_E(k)$ distribution.[25,26] This $P_E(k)$ distribution for $HO_2 \rightarrow H + O_2$ was incorporated into the above isolated resonance model to see how statistical fluctuations in the state-specific rate constants affect the collision-averaged $k(\omega,E)$ and Lindemann−Hinshelwood thermal $k_{uni}(\omega,T)$ rate constants for HO_2 dissociation.[19] The difference between the two $k_{uni}(\omega,T)$ curves increases with decrease in temperature and was found to be as large as 30% at 100 K.

In recent work, the state-specific unimolecular dissociation reaction

$$HOCl \rightarrow OH + Cl \qquad (12)$$

has been the focus of numerous experimental[27−36] and theoretical studies.[37−53] The quantum dynamical calculations of Hauschildt et al.,[52] for the ground-state potential energy surface, determined the state-specific rate constants for $J = 0$ and energies up to 10 kcal/mol above the unimolecular threshold. Three quantum numbers may be assigned to many of the resonance states. Thus, this unimolecular dissociation is highly mode-specific, and as shown in Figure 1, at low energies, the resonance states have rate constants which vary by more than 7 orders of magnitude. The resonance states with a large amount of quanta in the H−O stretch mode are particularly long-lived.[50−52] In the work presented here, the state-specific quantum dynamical calculations of Hauschildt et al.[52] are incorporated into the above isolated resonance model for unimolecular dissociation to calculate the pressure-dependent thermal rate constants for HOCl $\rightarrow$ OH + Cl dissociation. The resulting $k_{uni}(\omega,T)$ curves are compared with those of RRKM theory and a microcanonical variational transition state theory model[54−56] for unimolecular bond rupture. These calculations only include states for $J = 0$ and, thus, should be viewed as a model study to investigate the effect of mode specificity on the thermal unimolecular dissociation of HOCl.

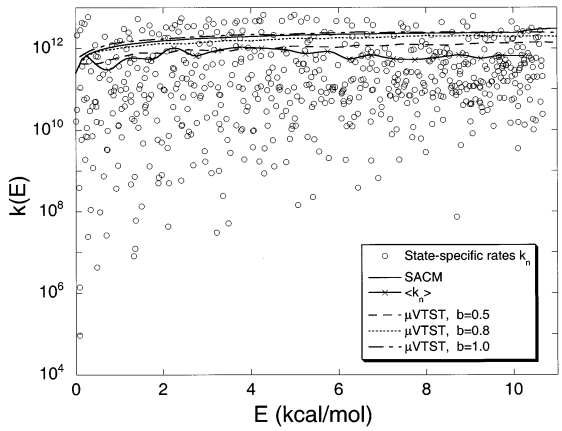

Figure 1. Unimolecular rate constants (s^{-1}) for HOCl $\rightarrow$ OH + Cl dissociation: o, quantum dynamical, state-specific rate constants of Hauschildt et al.;[52] (−x−), average of the state-specific rates with 0.5 kcal/mol energy width; (−), SACM vibrationally adiabatic rate constants; (−−−), (- - -) and (−-−) are microcanonical VTST rate constants with $b = 0.5$, 0.8, and 1.0 $Å^{-1}$, respectively (see text).

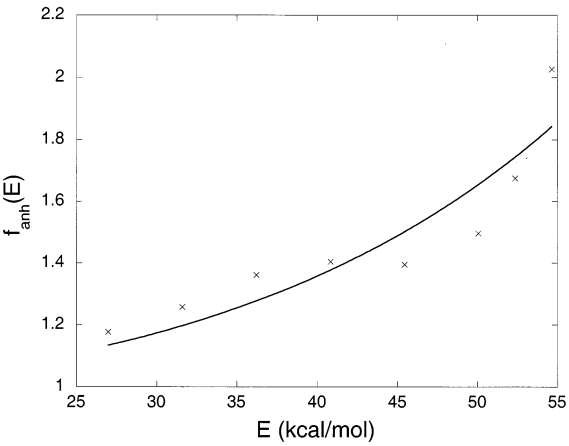

Figure 2. Comparison between the anharmonic correction to the HOCl density of states, i.e., $f_{anh}(E) = \rho_{anh}(E)/\rho_{har}(E)$, and the fit by eq 13. $\rho_{anh}(E)$ is determined from the quantum calculations of Hauschildt et al.[52]

II. HOCl Anharmonic Density of States

To calculate the $k_{uni}(\omega,T)$ rate constant for HOCl dissociation, an accurate density of states is required for the unimolecular reactant HOCl. From their quantum dynamical calculations, Hauschildt et al. determined the HOCl anharmonic density of states up to the zero-point corrected unimolecular dissociation threshold of 55.32 kcal/mol.[52] These densities of states are in excellent agreement with those deduced from experiment.[57] An anharmonic correction factor $f_{anh}(E)$ to the HOCl density of states may be determined by comparing the anharmonic and harmonic densities, i.e., $\rho_{anh}(E)$ and $\rho_{har}(E)$. The latter is determined from the HOCl harmonic vibrational frequencies, i.e., $\nu_{OH} = 3602.2\ cm^{-1}$, $\nu_{OCl} = 724.6\ cm^{-1}$, and $\nu_{bend} = 1238.3\ cm^{-1}$.[50] A plot of this $f_{anh}(E)$ correction factor is given in Figure 2.

To have a continuous expression for $f_{anh}(E)$, the points in Figure 2 were fit to the following model equation:[58]

$$f_{anh}(E) = \exp(bE^d)\left[1 + \frac{dbE^d}{s}\right] \qquad (13)$$

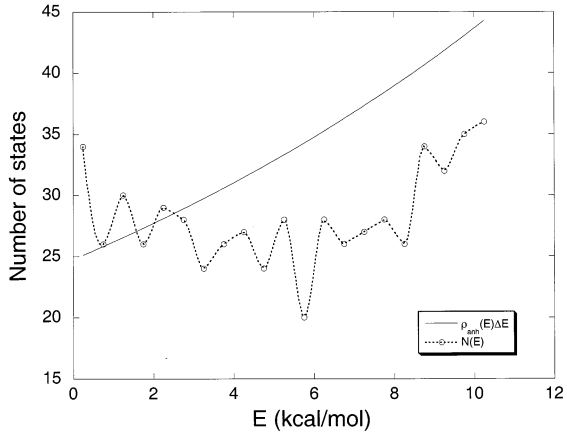

Figure 3. Comparison between $\rho_{anh}(E)\Delta E$, $\Delta E = 0.5$ kcal/mol, and the number of resonance states in the ΔE energy interval. $\rho_{anh}(E)$ is the fit from eq 13, and the latter is obtained by counting the number of states in Figure 1. E is the energy in excess of the unimolecular threshold.

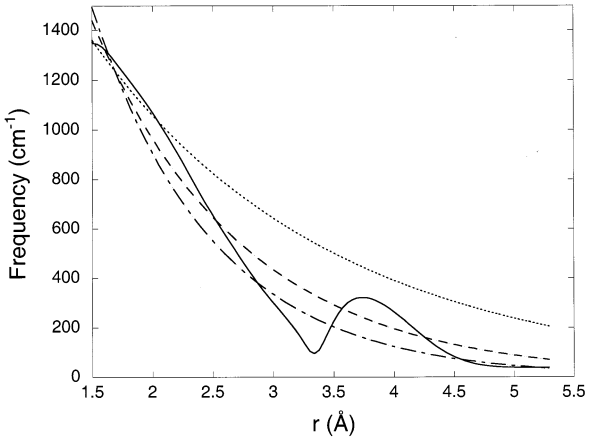

Figure 4. H−O- - -Cl bend frequency as a function of the O- - -Cl distance. (—), 1 ← 0 transition frequency from the vibrationally adiabatic potential energy curves; (·····), (- - -), and (- − -) are the curves from eq 15 with $b = 0.5$, 0.8, and 1.0 Å^{-1}, respectively.

where $s = 3$ is the number of vibrational degrees of freedom. The fitted values are $b = 3.72 \times 10^{-5}$ and $d = 2.30$. Here, parameter d is unitless, and b has a unit of (kcal/mol)$^{-d}$. As shown in Figure 2, the fit to the points is quite good. The extension of the anharmonic density of states, i.e., $\rho_{anh}(E) = f_{anh}(E)\rho_{har}(E)$, to energies above the unimolecular threshold is shown in Figure 3. Here, $\rho_{anh}(E)\Delta E$, with $\Delta E = 0.5$ kcal/mol, is compared with the actual number of resonance states in the ΔE energy interval.[52] The latter was obtained by counting the number of states in Figure 1 within ΔE. It should be noted that Troe[59] has proposed an empirical formula for the anharmonic density of states, which gives excellent fits to the experimental $\rho_{anh}(E)$ for HOCl[57] and NO_2.[60]

Overall, the anharmonic-corrected density of states above the unimolecular threshold is in good agreement with the quantum dynamical number of resonance states. The difference observed is that the number of resonance states identified in the quantum calculations falls somewhat below the number predicted by extending the anharmonic bound-state density above threshold. This is the direction in which one would expect any difference to occur, because it may be difficult to identify all of the broad, short-lived resonances in the quantum dynamical calculation and some of them may not be included in Figure 1. At the same time, the upper limit of the calculated rates in Figure 1 is well defined. It corresponds to the inverse time of a ballistic particle with energy E to move across the interaction zone of the potential energy surface.[50] Thus, the small discrepancy between the quantum results and the model predictions in Figure 3 may also be attributed to the limitations of the anharmonic density extrapolations.

III. Microcanonical Rate Constants and RRKM Model

A RRKM model is needed to calculate a $k_{uni}(\omega,T)$ curve to compare with that determined from the state-specific unimolecular rates. However, before presenting this model, it is useful to compare the HOCl → OH + Cl $k(E)$ curve determined previously[52] from the statistical adiabatic channel model (SACM)[61] with the curve of the average state-specific rates. Both of these curves are shown in Figure 1 and, except for the lowest energies, the average state-specific rates are significantly lower than the SACM rates. These average rates are determined for an energy interval of 0.5 kcal/mol, and the SACM rates are determined from the vibrationally adiabatic curves derived[52] from the HOCl → OH + Cl potential energy surface used in the quantum dynamical calculation. As discussed in the previous section, some of the broad resonances, with large rate constants, may not be included in Figure 1. Including these rates would increase the quantum average. On the other hand, the fact that the SACM rate is larger than the average of the state-specific rates is not unexpected, because the statistical hypothesis is not fulfilled for HOCl dissociation.

A variational RRKM model,[62] similar to that used previously[54−56] was developed for HOCl → OH + Cl dissociation. The model assumes that the OH stretch frequency remains constant at 3602 cm^{-1} as the O−Cl bond ruptures. The reaction coordinate potential is modeled by the Morse function

$$V(r) = D_e[1 - e^{-\beta_e(r - r_e)}]^2 - D_e \qquad (14)$$

where D_e is the classical O−Cl bond dissociation energy. The values for the parameters in eq 14 are $D_e = 58.30$ kcal/mol, $r_e = 1.689$ Å, and $\beta_e = 2.09$ Å^{-1}. The attenuation of the H−O- - -Cl bending frequency, as the O−Cl bond ruptures, is represented by

$$\nu(r) = \nu_e \exp[-b(r - r_e)] \qquad (15)$$

where $\nu_e = 1238$ cm^{-1} is the bend frequency at the HOCl potential energy minimum. The b term in eq 15 is the only adjustable parameter in this variational RRKM model for HOCl dissociation.

The microcanonical variational RRKM rate constants were calculated using the expression

$$k(E) = \frac{N^{\ddagger}(E)}{h\rho(E)} \qquad (16)$$

where $N^{\ddagger}(E)$ is the minimum in the sum of states along the O−Cl dissociation reaction path and $\rho(E)$ is the HOCl anharmonic density of states, as described above. RRKM $k(E)$ curves, determined with the b parameter in eq 15 set to 0.5, 0.8, and 1.0 Å^{-1}, are shown in Figure 1. The SACM curve is in good agreement with the $b = 0.8$ Å^{-1} curve at low energies and the $b = 1.0$ Å^{-1} curve at intermediate and high energies. The $b = 0.5$ Å^{-1} curve is in good agreement with the averages of the state-specific rates. The curves of the H−O- - -Cl bending frequency versus the H−O- - -Cl distance r, for $b = 0.5$, 0.8, and 1.0 Å^{-1}, are given in Figure 4. Also shown is the plot of

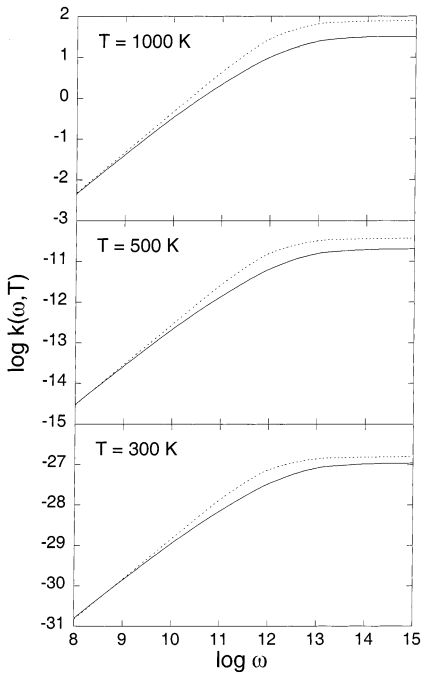

Figure 5. Plots of $k_{uni}(\omega,T)$ for the isolated resonance state-specific model (—), eq 9, and the variational RRKM model (- - -), eq 10, with bend attenuation parameter $b = 1.0$ Å^{-1}.

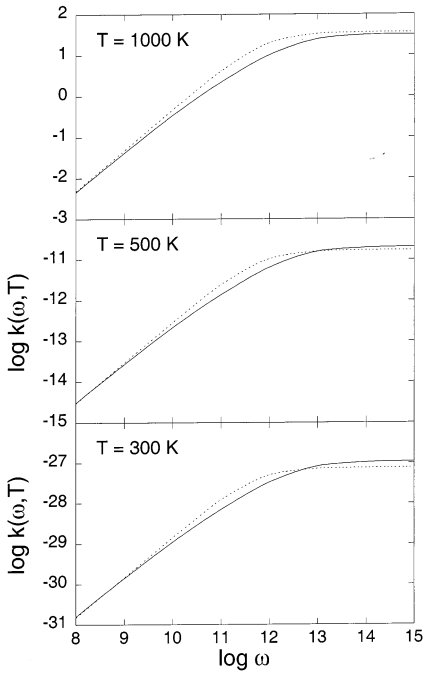

Figure 6. Same as Figure 5, except $b = 0.5$ Å^{-1}.

the $1 \leftarrow 0$ transition frequency for the H−O- - -Cl bend, determined from the vibrationally adiabatic potential energy curves for the HOCl → OH + Cl analytic potential energy surface.[52]

IV. Lindemann−Hinshelwood Thermal Unimolecular Rate Constant $k_{uni}(\omega,T)$

Both the isolated resonance, eq 9, and RRKM, eq 10, models are used to calculate $k_{uni}(\omega,T)$. To evaluate eq 9, the resonance rates k_n and energies E_n are taken from Figure 1 and the partition function Q is calculated from the anharmonic energy levels calculated by Hauschildt et al.[52] for HOCl. Equation 10 is evaluated by using the variational RRKM $k(E)$ discussed in the previous section for $k(\omega,E)$, the anharmonic density of states $\rho_{anh}(E)$ for $\rho(E)$, and the same Q as above. It is noteworthy that the harmonic approximation is excellent for evaluating Q, because the harmonic and anharmonic Q differ by less than 1% at 1000 K.

A. Variational RRKM Model with $b = 1.0$ Å^{-1}. Figure 5 gives a comparison of the state-specific $k_{uni}(\omega,T)$ curve with that calculated for the variational RRKM model with $b = 1.0$ Å^{-1}. As shown in Figure 1, this variational RRKM model gives a good representation of the SACM $k(E)$ curve, which is calculated from the vibrationally adiabatic potential energy curves for the analytic potential energy surface used to determine the resonance rates and energies. Thus, Figure 5 also represents a comparison of the $k_{uni}(\omega,T)$ curve of the SACM model with that for the actual quantum dynamics, with both curves based on the same potential energy surface.

As shown in Figure 5, the state-specific $k_{uni}(\omega,T)$ is a factor of 2.0−2.4 smaller than the RRKM value at the high-pressure limit. This is because the high-pressure limiting rate is a Boltzmann weighting of the energy and state-dependent rate constants and, as shown in Figure 1, the RRKM $k(E)$ for $b = 1.0$ Å^{-1} and the SACM $k(E)$ are significantly larger than the energy-dependent average of the state-specific rates. At low pressure, the two $k_{uni}(\omega,T)$ curves are nearly identical, as expected, because in the low pressure limit the rate constant is proportional to the Boltzmann weighted density of reacting states, which is nearly the same for the two models.

B. Variational RRKM Model with $b = 0.5$ Å^{-1}. A RRKM model is often constructed to fit the experimental high-pressure $k_{uni}(\omega,T)$ rate constant, and this model is then used to calculate the complete $k_{uni}(\omega,T)$ versus ω curve for comparison with experiment. As shown in Figure 1, the decomposition of HOCl is state-specific, and the $k_{uni}(\omega,T)$ curve calculated with the state-specific model should represent the experimental $k_{uni}(\omega,T)$ curve. An approach akin to fitting the experiment is to choose a RRKM model which fits the state-specific high-pressure $k_{uni}(\omega,T)$ rates. The variational RRKM model with $b = 0.5$ Å^{-1} is expected to give an approximate fit to the state-specific high-pressure $k_{uni}(\omega,T)$, because this RRKM model gives $k(E)$ rate constants in approximate agreement with the averages of the state-specific rates (e.g., see Figure 1).

The $k_{uni}(\omega,T)$ curves calculated with the $b = 0.5$ Å^{-1} variational RRKM model are compared with the state-specific $k_{uni}(\omega,T)$ curves in Figure 6. The two sets of high-pressure rate constants are in approximate agreement. However, at intermediate pressures, the state-specific curve is significantly lower than the RRKM one. For $T = 1000$ K, where the two sets of curves are nearly the same at high-pressure, the state-specific curve is as much as a factor of 2.0 lower at intermediate pressures. If the curves for 300 and 500 K are shifted so that they agree at high-pressures, a similar lowering of the state-specific $k_{uni}(\omega,T)$ curve is found for these temperatures. Thus, the effect of the orders-of-magnitude differences in the state-specific rates shown in Figure 1 is to give a state-specific $k_{uni}(\omega,T)$ curve which is a factor of 2.0 lower than the standard RRKM one at intermediate pressure. This is a significant effect and should be observable when fitting the experimental $k_{uni}(\omega,T)$ curve for HOCl → OH + Cl dissociation. In the Appendix, it is shown that, if the RRKM rate constant $k(E)$ equals $\langle k_n \rangle$, the average of the state-specific rates for the energy interval E to $E + \Delta E$, the RRKM $k_{uni}(\omega,T)$ will always be larger than the state-specific $k_{uni}(\omega,T)$.

V. Discussion

The calculations reported here and those of previous studies provide detailed information concerning the relationship between state specific and thermal unimolecular rate constants for the $J = 0$ dissociation reaction HOCl → OH + Cl. The findings of these studies are reviewed in the following.

Vibrationally adiabatic potential energy curves have been calculated for the potential energy surface used in the quantum dynamical calculation of the state-specific rate constants for HOCl dissociation,[52] and microcanonical statistical adiabatic channel model (SACM) unimolecular rate constants have been calculated from these curves. High-pressure thermal unimolecular rate constants $k_{uni}(\omega,T)$, determined from these SACM $k(E)$ rate constants, are a factor of 2 or more higher than $k_{uni}(\omega,T)$ determined from the state-specific rates. However, it is difficult to identify all of the broad resonances with large rate constants in the quantum dynamical calculations and, if some of these resonances are not included in Figure 1, the actual state-specific $k_{uni}(\omega,T)$ will be larger and may be in better agreement with the SACM $k_{uni}(\omega,T)$. It is of interest that the SACM $k(E)$ may be fit by a simple variational RRKM model,[54−56] for which the HO- - -Cl bend frequency is attenuated exponentially as the O- - -Cl bond ruptures. This attenuated bend frequency is similar to the $1 \leftarrow 0$ transition frequency for the bend determined from the vibrationally adiabatic potential energy curves.

In contrast to the high-pressure rate constants, in the low-pressure limit, the state-specific, RRKM, and SACM $k_{uni}(\omega,T)$ agree, because in this limit the rate constant is proportional to the collision frequency and the Boltzmann weighted density of reacting states, which is nearly the same for the three models. A variational RRKM model may be chosen to fit the state-specific value of $k_{uni}(\omega,T)$ in the high-pressure limit. However, at intermediate pressures, this model gives values for $k_{uni}(\omega,T)$ which are as much as a factor of 2 larger than the state-specific values.

A unimolecular model with nonexponential decay, at each energy, is required to fit the state-specific $k_{uni}(\omega,T)$. A RRKM model with reduced dimensionality (i.e., a model with only a fraction of the reaction phase space coupled to the dissociation coordinate),[63] but one that retains exponential decay, cannot be adjusted to fit the state-specific $k_{uni}(\omega,T)$ curve. The quantum dynamics for HOCl → OH + Cl dissociation suggests that the phase space of the HOCl reactant consists of chaotic, quasi-periodic, and vague tori[64,65] trajectories, as has been found for the model HCC → H + C═C reaction.[13,66,67] Such a phase space structure will give rise to nonexponential classical unimolecular dissociation for a microcanonical ensemble of HOCl initial states. It is of interest to investigate the classical phase space structure and classical unimolecular dynamics of HOCl. A study of the phase space structure for a two-dimensional model of HOCl has been completed.[49]

Finally, it should be emphasized that the state-specific rate constants used in the calculations of $k_{uni}(\omega,T)$ reported here are for total angular momentum $J = 0$. The reactant density of states will increase by including resonance states with $J > 0$, but this will not necessarily alter the difference found here between the RRKM and state-specific $k_{uni}(\omega,T)$ curves for $J = 0$. However, if there is significantly more coupling and less mode-specificity for the resonance states with $J > 0$, this may result in less fluctuations in the state-specific resonance rates and, as a result, better agreement between the RRKM and state-specific $k_{uni}(\omega,T)$ curves.[2,6] In future work, it will be of much interest to investigate the effect of total angular momentum on the thermal unimolecular rate constant for HOCl dissociation.

Acknowledgment. This research was supported by the National Science Foundation. The authors wish to acknowledge important discussions with Jürgen Troe. The research of Don Setser and that of Don Setser and Seymour Rabinovitch has taught the authors very much about unimolecular dynamics and kinetics and has provided a foundation for much of their research. The authors are honored to have the opportunity to contribute to this special issue.

Appendix

It can be shown that the state-specific $k_{uni}(\omega,E)$ in eq 8 is smaller than the RRKM-type $k_{uni}(\omega,E)$ given by

$$k_{uni}(\omega,E) = \frac{\omega\langle k_n\rangle}{\langle k_n\rangle + \omega} \tag{A1}$$

when $\langle k_n\rangle$ is the average of the state-specific rate constants k_n. Thus, if $\langle k_n\rangle$ equals the RRKM rate constant $k(E)$, which may be the case for many unimolecular dissociations,[68,69] the RRKM $k_{uni}(\omega,E)$ is larger than the state-specific value.

The problem is to prove that

$$\frac{\langle k\rangle}{\langle k\rangle + \omega} \geq \frac{1}{N}\sum_{i=1}^{N}\frac{k_i}{k_i + \omega} \tag{A2}$$

$$1 - \frac{\omega}{\langle k\rangle + \omega} \geq \frac{1}{N}\sum_{i=1}^{N}\left(1 - \frac{\omega}{k_i + \omega}\right) = 1 - \frac{1}{N}\sum_{i=1}^{N}\frac{\omega}{k_i + \omega} \tag{A3}$$

and, thus

$$\frac{1}{\langle k\rangle + \omega} \leq \frac{1}{N}\sum_{i=1}^{N}\frac{1}{k_i + \omega} \tag{A4}$$

If one sets $x_i = k_i + \omega$, the problem reduces to

$$\frac{1}{\langle x\rangle} \leq \frac{1}{N}\sum_{i=1}^{N}\frac{1}{x_i} \tag{A5}$$

It is straightforward to show that eq A5 is true for $N = 2$, for which $\langle x\rangle = (x_1 + x_2)/2$. For $N = 2$, eq A5 becomes

$$\frac{2}{x_1 + x_2} \leq \frac{1}{2}\left(\frac{1}{x_1} + \frac{1}{x_2}\right) = \frac{x_1 + x_2}{2x_1x_2} \tag{A6}$$

If both sides of eq A6 are multiplied by $2x_1x_2(x_1 + x_2)$, one has $(x_1 + x_2)^2 \geq 4x_1x_2$. This can be rearranged to $(x_1 - x_2)^2 \geq 0$, which is true for all positive x_i's.

Suppose eq A5 is true for $N = n$, as shown above for $N = 2$. One can then prove the general validity of eq A5, by proving it is also valid for $N = n + 1$. For $N = n + 1$, eq A5 becomes

$$\frac{(n+1)}{\sum_{i=1}^{n}x_i + x_{n+1}} \leq \frac{1}{n+1}\left(\sum_{i=1}^{n}\frac{1}{x_i} + \frac{1}{x_{n+1}}\right) \tag{A7}$$

which after expanding, may be written as

$$\sum_{i=1}^{n} x_i \cdot \sum_{i=1}^{n} \frac{1}{x_i} + \frac{1}{x_{n+1}} \sum_{i=1}^{n} x_i + x_{n+1} \sum_{i=1}^{n} x_i + 1 \geq (n+1)^2 \quad \text{(A8)}$$

Because it is assumed that eq A5 holds for $N = n$, the first term is greater than or equal to n^2. Hence, eq A8 becomes

$$\frac{1}{x_{n+1}} \sum_{i=1}^{n} x_i + x_{n+1} \sum_{i=1}^{n} \frac{1}{x_i} \geq 2n$$

$$\sum_{i=1}^{n} \left(\frac{x_i}{x_{n+1}} + \frac{x_{n+1}}{x_i} \right) \geq 2n \quad \text{(A9)}$$

Using the fact that $(x_i - x_{n+1})^2 \geq 0$, one can show

$$\frac{x_i}{x_{n+1}} + \frac{x_{n+1}}{x_i} = \frac{x_i^2 + x_{n+1}^2}{x_i x_{n+1}} \geq 2 \quad \text{(A10)}$$

If eq A10 is summed over $i = 1$ to n, one has proven that eq A5 holds for all N. Thus, $k_{\text{uni}}(\omega,E)$ determined from eq A1 is larger than that found from eq 8.

References and Notes

(1) Rabinovitch, B. S.; Setser, D. W. *Adv. Photochem.* **1964**, *3*, 1.
(2) Baer, T.; Hase, W. L. *Unimolecular Reaction Dynamics. Theory and Experiments*; Oxford University Press: New York, 1996.
(3) Mies, F. H.; Krauss, M. *J. Chem. Phys.* **1966**, *45*, 4455.
(4) Mies, F. H. *J. Chem. Phys.* **1969**, *51*, 798.
(5) Wagner, A. F.; Bowman, J. M. *J. Phys. Chem.* **1987**, *91*, 5314.
(6) Hase, W. L.; Cho, S.-W.; Lu, D.-h.; Swamy, K. N. *Chem. Phys.* **1989**, *139*, 1.
(7) Polik, W. F.; Moore, C. B.; Miller, W. H. *J. Chem. Phys.* **1988**, *89*, 3584.
(8) Polik, W. F.; Guyer, D. R.; Miller, W. H.; Moore, C. B. *J. Chem. Phys.* **1990**, *92*, 3471.
(9) Someda, K.; Nakamura, H.; Mies, F. H. *Chem. Phys.* **1994**, *187*, 195.
(10) Someda, K.; Nakamura, H.; Mies, F. H. *Prog. Theor. Phys. Suppl.* **1994**, *116*, 443.
(11) Peskin, U.; Reisler, H.; Miller, W. H. *J. Chem. Phys.* **1994**, *101*, 9672.
(12) Peskin, U.; Miller, W. H.; Reisler, H. *J. Chem. Phys.* **1995**, *102*, 8874.
(13) Hase, W. L.; Duchovic, R. J.; Swamy, K. N.; Wolf, R. J. *J. Chem. Phys.* **1984**, *80*, 714.
(14) Lu, D.-h.; Hase, W. L. *J. Chem. Phys.* **1989**, *90*, 1557.
(15) Lu, D.-h.; Hase, W. L. *J. Phys. Chem.* **1989**, *93*, 1681.
(16) Slater, N. B. *Theory of Unimolecular Reactions*; Cornell University Press: Ithaca, NY, 1959.
(17) Bunker, D. L. *J. Chem. Phys.* **1964**, *40*, 1946.
(18) Miller, W. H. *J. Phys. Chem.* **1988**, *92*, 4261.
(19) Song, K.; Hase, W. L. *J. Phys. Chem. A* **1998**, *102*, 1292.
(20) Dobbyn, A. J.; Stumpf, M.; Keller, H.-M.; Schinke, R. *J. Chem. Phys.* **1995**, *103*, 9947.
(21) Dobbyn, A. J.; Stumpf, M.; Keller, H.-M.; Hase, W. L.; Schinke, R. *J. Chem. Phys.* **1995**, *102*, 5867.
(22) Dobbyn, A. J.; Stumpf, M.; Keller, H.-M.; Schinke, R. *J. Chem. Phys.* **1996**, *104*, 8357.
(23) Kendrick, B. K.; Pack, R. T. *Chem. Phys. Lett.* **1995**, *235*, 291.
(24) Mandelshtam, V. A.; Grozdanov, T. P.; Taylor, H. S. *J. Chem. Phys.* **1995**, *103*, 10074.
(25) Levine, R. D. *Ber. Bunsen-Ges. Phys. Chem.* **1988**, *92*, 222.
(26) Porter, C. E.; Thomas, R. G. *Phys. Rev.* **1956**, *104*, 483.
(27) Jungkamp, T. P. W.; Kerchner, U.; Schmidt, M.; Schindler, R. N. *J. Photochem. Photobiol. A: Chemistry* **1995**, *91*, 1.
(28) Schindler, R. N.; Liesner, M.; Schmidt, S.; Kirchner, U.; Benter, T. *J. Photochem. Photobiol. A: Chemistry* **1997**, *107*, 9.
(29) Dutton, G.; Barnes, R. J.; Sinha, A. *J. Chem. Phys.* **1999**, *111*, 4976.
(30) Barnes, R. J.; Sinha, A. *J. Chem. Phys.* **1997**, *107*, 3730.
(31) Barnes, R. J.; Dutton, G.; Sinha, A. *J. Phys. Chem. A* **1997**, *101*, 8374.
(32) Tanaka, Y.; Kawasaki, M.; Matsumi, Y.; Fujiwara, H.; Ishiwata, T.; Rogers, L. J.; Dixon, R. N.; Ashfold, M. N. R. *J. Chem. Phys.* **1998**, *109*, 1315.
(33) Callegari, A.; Rebstein, J.; Muenter, J. S.; Jost, R.; Rizzo, T. R. *J. Chem. Phys.* **1999**, *111*, 123.
(34) Callegari, A.; Rebstein, J.; Jost, R.; Rizzo, T. R. *J. Chem. Phys.* **1999**, *111*, 7359.
(35) Callegari, A.; Rebstein, J.; Muenter, J. S.; Jost, R.; Rizzo, T. R. *J. Chem. Phys.* **2000**, *112*, 2569.
(36) Wedlock, M. R.; Jost, R.; Rizzo, T. R. *J. Chem. Phys.* **1997**, *107*, 10344.
(37) Weiss, J.; Hauschildt, J.; Schinke, R.; Haan, O.; Skokov, S.; Bowman, J. M.; Mandelshtam, V. A.; Peterson, K. A. *J. Chem. Phys.* **2001**, *115*, 8880.
(38) Escribano, R. M.; Di Lonardo, G.; Fusina, L. *Chem. Phys. Lett.* **1996**, *259*, 614.
(39) Peterson, K. A. *Spectrochim. Acta A* **1997**, *53*, 1051.
(40) Koput, J.; Peterson, K. A. *Chem. Phys. Lett.* **1998**, *283*, 139.
(41) Skokov, S.; Peterson, K. A.; Bowman, J. M. *J. Chem. Phys.* **1998**, *109*, 2662.
(42) Skokov, S.; Qi, J.; Bowman, J. M.; Yang, C.-Y.; Gray, S. K.; Peterson, K. A.; Mandelshtam, V. A. *J. Chem. Phys.* **1998**, *109*, 10273.
(43) Skokov, S.; Peterson, K. A.; Bowman, J. M. *Chem. Phys. Lett.* **1999**, *312*, 494.
(44) Skokov, S.; Bowman, J. M.; Mandelshtam, V. A. *Phys. Chem. Chem. Phys.* **1999**, *1*, 1279.
(45) Peterson, K. A.; Skokov, S.; Bowman, J. M. *J. Chem. Phys.* **1999**, *111*, 7446.
(46) Skokov, S.; Bowman, J. M. *J. Chem. Phys.* **1999**, *110*, 9789.
(47) Chen, R.; Guo, H. *Chem. Phys. Lett.* **1999**, *308*, 123.
(48) Zhang, H.; Ramachandran, B.; Senekowitch, J.; Wyatt, R. E. *J. Mol. Struct. (THEOCHEM)* **1999**, *487*, 75.
(49) Joyeux, M.; Sugny, D.; Lombardi, M.; Jost, R.; Schinke, R.; Skokov, S.; Bowman, J. M. *J. Chem. Phys.* **2000**, *113*, 9610.
(50) Weiss, J.; Hauschildt, J.; Grebenshchikov, S. Y.; Düren, R.; Schinke, R.; Koput, J.; Stamatiadis, S.; Farantos, S. C. *J. Chem. Phys.* **2000**, *112*, 77.
(51) Hauschildt, J.; Weiss, J.; Schinke, R. *Z. Phys. Chem.* **2000**, *214*, 609.
(52) Hauschildt, J.; Weiss, J.; Beck, C.; Grebenshchikov, S. Y.; Düren, R.; Schinke, R.; Koput, J. *Chem. Phys. Lett.* **1999**, *300*, 569.
(53) Zou, S.; Skokov, S.; Bowman, J. M. *Chem. Phys. Lett.* **2001**, *339*, 290.
(54) Hase, W. L. *J. Chem. Phys.* **1972**, *57*, 730.
(55) Hase, W. L. *Chem. Phys. Lett.* **1987**, *139*, 389.
(56) Hu, X.; Hase, W. L. *J. Phys. Chem.* **1989**, *93*, 6029.
(57) Abel, B.; Hamann, H. H.; Kachanov, A. A.; Troe, J. *J. Chem. Phys.* **1996**, *104*, 3189.
(58) Song, K.; Hase, W. L. *J. Chem. Phys.* **1999**, *110*, 6198.
(59) Troe, J. *Chem. Phys.* **1995**, *190*, 381.
(60) Saltzgeber, R. F.; Mandelshtam, V. A.; Schlier, C.; Taylor, H. S. *J. Chem. Phys.* **1999**, *110*, 3756.
(61) Quack, M.; Troe, J. *Ber. Bunsen-Ges. Phys. Chem.* **1974**, *78*, 240.
(62) Hase, W. L. *Acc. Chem. Res.* **1983**, *16*, 258.
(63) Hase, W. L.; Buckowski, D. G.; Swamy, K. N. *J. Phys. Chem.* **1983**, *87*, 2754.
(64) Reinhardt, W. P. *J. Phys. Chem.* **1982**, *86*, 2158.
(65) Shirts, R. B.; Reinhardt, W. P. *J. Chem. Phys.* **1982**, *77*, 5204.
(66) Wolf, R. J.; Hase, W. L. *J. Chem. Phys.* **1980**, *73*, 3779.
(67) Duchovic, R. J.; Swamy, K. N.; Hase, W. L. *J. Chem. Phys.* **1984**, *80*, 1462.
(68) Waite, B. A.; Miller, W. H. *J. Chem. Phys.* **1980**, *73*, 3713.
(69) Reference 2, page 292.